Mixed Cations for the Stabilization of New Features. $Ca_{6.2}Mg_{3.8}Sn_7$, a Phase with Planar Zigzag Chains of Interlinked Square-Planar Tin Units

Ashok K. Ganguli,[†,‡] John D. Corbett,*[,‡] and Martin Köckerling[§]

Contribution from the Ames Laboratory-DOE[1] and Department of Chemistry, Iowa State University, Ames, Iowa 50011, and FB6-Festkörperchemie, Gerhard-Mercator-Universität, 47057 Duisburg, Germany

Received August 11, 1997

Abstract: The structure of orthorhombic $Ca_{6.24(6)}Mg_{3.76(6)}Sn_7$ contains two types of chains built from edge- or face-sharing trigonal prisms of Ca and Mg atoms that are centered by Sn atoms. In one type, bonded zigzag $^1_\infty[Sn_5^{12-}]$ chains are built of interconnected square-planar (D_{2h}) Sn_5 units. Alternating chains of condensed trigonal prismatic cations centered by isolated Sn atoms are interbonded to the first type through Sn−Ca,Mg interactions. The chain unit is two electrons richer than that for a simple Zintl−Klemm formalism for 1-, 2-, and 4-bonded Sn (4b-Sn^0) because of the square-planar tin bonding. Band structure calculations within the extended Hückel formalism indicate the infinite tin chain alone is closed shell, but a metallic behavior (via open π-bonding) is produced by cation mixing in the full structure. Local bonding within square-planar Sn_5 consists of normal s, p_x, p_y (σ) bonding, a single 4c-2e nonbonding MO on the outer tins, and a p_z^2 lone (π) pair. This new intermediate degree of hypervalency makes the unit isoelectronic with XeF_4^{2+}. Property studies on powdered samples reveal a good metallic conduction but a small diamagnetism that is not uncharacteristic of heavy p-elements and their compounds.

Introduction

Much of the foundation of solid-state inorganic chemistry comes from the multitudinous crystal structures that have been defined, the elements that may be involved for each, the characteristic properties of each phase such as conduction and magnetism, and what we can understand and categorize about the bonding in each phase or structure type. And the structure of solid-state chemistry is still very much in its youth as far as the ability to predict what compounds and structures are possible. Thus exploratory synthesis remains an essential and active endeavor that is at the same time often exciting and challenging because of the numerous unprecedented, even inconceivable, compounds that can be found. The present article reports such a discovery made in the course of simply trying to "fill out" a family of compositions and structures.

Phases with A_5B_3 compositions span a wide variety of elements, structures, and chemistries. Those for A = Ca, Sr, Ba, Zr and B = Sb, Bi, Sn, Pb have been the focus of solid-state research for some time.[2−4] Most of the binary phases crystallize in either the hexagonal Mn_5Si_3-type or the tetragonal Cr_5B_3-type structures. On the other hand, no pair of the above elements appears to form a binary compound with the W_5Si_3 structure, although a few ternary substitutional derivatives are known.[5,6] The Mn_5Si_3 structure type is well-known as an excellent host for a wide variety of interstitial atoms that afford "stuffed" A_5B_3Z analogues.[7−10] Recently, Cr_5B_3-type examples for Ca, Sr, Sn, Pb have also been shown to form interstitial derivatives, or to exist only as ternary phases, especially with H or F.[11,12]

A noteworthy exception in this A_5B_3 family has been the absence of any Ca_5Sn_3 example, for which the unusual stability of the nearby $Ca_{31}Sn_{20}$ has been offered as one explanation.[13] The presence of several oligomeric polytin anions in the latter compound brings to attention another fairly recent feature of tin chemistry, its considerable tendency to form Sn−Sn bonds in diverse anionic states, viz., in K_8Sn_{25}, K_8Sn_{44},[14,15] $Yb_{36}Sn_{23}$,[11] $NaGaSn_2$,[16] $(Na\text{-crypt}^+)_4Sn_9^{4-}$,[17] and others.

The genesis of the present exploration was an attempt to prepare a derivative of the unknown W_5Si_3-type Ca_5Sn_3. This structure has an inherent problem of short A−A separations along the tetrahedral chains that lie on the side faces of the

† Permanent address: Department of Chemistry, Indian Institute of Technology, New Delhi 110016, India.
‡ Iowa State University.
§ Gerhard-Mercator-Universität.

(1) This research was supported by the Office of the Basic Energy Sciences, Materials Science Division, U.S. Department of Energy. The Ames Laboratory is operated for the DOE by Iowa State University under Contract No. W-7405-Eng-82.

(2) Dorrscheidt, W.; Widera, A.; Schäfer, H. *Z. Naturforsch.* **1977**, *32B*, 1097.
(3) Bruzzone, G.; Franceschi, E.; Merlo, F. *J. Less-Common Met.* **1978,** *60*, 59.
(4) Pearson, W. B. *The Crystal Chemistry and Physics of Metals and Alloys*; Wiley-Interscience: New York, 1972; p 731.
(5) Kwon, Y.-U.; Sevov, S. C.; Corbett, J. D. *Chem. Mater.* **1990**, *2*, 550.
(6) Ganguli, A. K.; Corbett, J. D. To be submitted for publication.
(7) Hurng, W.-M.; Corbett, J. D. *Chem. Mater.* **1989**, *1*, 311.
(8) Garcia, E.; Corbett, J. D. *Inorg. Chem.* **1990**, *29*, 3274.
(9) Kwon, Y.-U.; Corbett, J. D. *Chem. Mater.* **1992**, *4*, 1348.
(10) Guloy, A. M.; Corbett, J. D. *J. Solid State Chem.* **1994**, *109*, 352.
(11) Leon-Escamilla, E. A. Ph.D. Dissertation, Iowa State University, 1996.
(12) Leon-Escamilla, E. A.; Corbett, J. D. *J. Alloys Compd.* In press.
(13) Ganguli, A. K.; Guloy, A. M.; Leon-Escamilla, E. A.; Corbett, J. D. *Inorg. Chem.* **1993**, *32*, 4349.
(14) Zhao, J.-T.; Corbett, J. D. *Inorg. Chem.* **1994**, *33*, 5721.
(15) von Schnering, H.-G. Private communications.
(16) Vaughey, J. T.; Corbett, J. D. *J. Am. Chem. Soc.* **1997**, *118*, 12098.
(17) Corbett, J. D.; Edwards, P. A. *J. Am. Chem. Soc.* **1977**, *99*, 3313.

S0002-7863(97)02812-6 CCC: $15.00 © 1998 American Chemical Society
Published on Web 02/03/1998

tetragonal cell, and partial substitution of a smaller cation like Mg^{2+} seemed appropriate. We did obtain such a tetragonal W_5Si_3-type product, but with an unexpected substitution mode.[6] But the more novel result was the second compound discovered in the process, $Ca_{6.2}Mg_{3.8}Sn_7$. This phase demonstrates not only the striking effect that different cations can have on phase stability but also the existence of an unprecedented type of infinite tin chain constructed from square-planar tin units. In this paper we describe the synthesis, crystal structure, properties, and bonding of this remarkable phase.

Experimental Section

Syntheses. Stoichiometric amounts of Ca (99.99%, Applied Physics Lab), Mg (99.99%, Ames Lab.), and Sn (99.99%, Baker; clean on fusion) to give various $(Ca,Mg)_5Sn_3$ compositions were weighed into Ta tubes in a He-filled glovebox. The tubes were arc-welded shut and then sealed in well-baked, evacuated silica tubes. The new phase was readily evident in the powder patterns of the first products, and a single crystal for structure determination was picked from a reaction loaded as Ca_4MgSn_3. Since thermodynamic equilibrium is obtained at the temperatures used, new compositions determined by X-ray means are customarily verified by their subsequent synthesis in high yields from reactions with the indicated stoichiometry. Such a sample heated at 925 °C for 6 h, then cooled to 600 °C and annealed for 6 days gave 85% of the subject phase. Yields up to ~95% (the remainder being Sn) could be obtained when the stoichiometric composition was first heated to 925 °C for 6 h and quenched in water to give a homogeneous sample. After grinding, this was loaded into a fresh Ta tube, which was welded, sealed into an evacuated silica jacket, and then further annealed for 6 days at 600 °C. Shiny surfaces on crystals of the new phase turn dull gray immediately on exposure to air.

X-ray powder diffraction patterns were obtained as usual[7−10] from samples mounted on a frame between pieces of cellophane tape in the glovebox so as to protect them from the atmosphere. An Enraf-Nonius Guinier camera with Cu Kα radiation and NIST reference Si as an internal standard were employed to obtain useful powder diffraction data. The known 2θ values of the standard lines were fit to a quadratic in their measured positions on the film, and lattice constants of the sample then calculated by the least-squares fit to ~34 measured and indexed lines.

Structural Study. A shiny black, bar-shaped crystal ~0.12 × 0.05 × 0.03 mm was mounted in a glass capillary inside the glovebox. The crystal was first checked with oscillation photographs and then transferred to an automatic diffractometer (Rigaku AFC6R) for data collection, which took place at room temperature with monochromated Mo Kα radiation. The diffraction data were corrected for Lorentz and polarization effects and for absorption with the aid of the average of three Ψ-scans made on reflections with different 2θ values.

The centrosymmetric space group *Pbam* was chosen for the structure refinement on the basis of systematic absences, the statistical N(Z) test, and the Laue group indicated by the TEXSAN program package.[18] Application of direct methods with SHELXS[19] revealed all Sn and some of the Ca atoms. A few cycles of least-squares refinement and a subsequent difference Fourier synthesis located the remaining atoms. The thermal parameter of one Mg atom was negative at this stage, but refinement of this with mixed Mg, Ca occupancy, keeping the total occupancy fixed at unity, led to an 88(3):12(3) proportion and a more reasonable thermal parameter. The final cycle of full-matrix, least-squares refinement with 457 observed reflections ($I > 3\sigma(I)$) and 55 variables (including all positional and anisotropic thermal parameters) converged at $R(F)/R_w = 0.027/0.027$. The refined composition is $Ca_{6.26(6)}Mg_{3.76(6)}Sn_7$. Some aspects of the data collection and refinement are listed in Table 1. More detailed crystallographic information as well as the anisotropic displacement parameters are available in Supporting Information. These as well as the F_o/F_c listing are also available from J.D.C.

Table 1. Some Data Collection and Refinement Parameters for $Ca_{6.24(6)}Mg_{3.76(6)}Sn_7$

formula wt	1172.3
lattice parameters,[a] Å	$a = 7.794(1)$, $b = 25.718(4)$, $c = 4.655(1)$
V, Å^3	932.9(5)
space group; Z	*Pbam* (No. 55); 2
d_{calc}, g/cm^3	4.173
μ, cm^{-1} (Mo Kα)	110.41
R, R_w[b]	0.027, 0.027

[a] From Guinier powder data, $\lambda = 1.540\,562$ Å, 23 °C. [b] $R = \sum||F_o| - |F_c||/\sum|F_o|$; $R_w = [\sum w(|F_o| - |F_c|)^2/\sum w(F_o)^2]^{1/2}$; $w = \sigma_F^{-2}$.

Table 2. Parameters for the Extended Hückel Calculations[23]

atom	orbital	H_{ii} (eV)	ζ
Sn	5s	−14.150	2.12
	5p	−7.311	1.82
Ca	4s	−6.564	1.20
	4p	−4.068	1.20
Mg	3s	−8.201	1.10
	3p	−4.641	1.10

Properties. Magnetic susceptibilities were measured on powdered samples held between the faces of two silica rods within a container sealed under He. Data were collected at 3T between 6 and 300 K on a Quantum Design MSPS SQUID magnetometer and corrected for core contributions. Resistivities were measured at 35 MHz and over 90−255 K by the "Q" method[20] on a finely powdered sample diluted with chromatographic Al_2O_3. The absolute resistivity values are believed to be correct within a factor of about three.

Band Calculations. Calculations by the extended Hückel tight-binding method[21,22] were done with the aid of the program EHMACC adapted to an IBM-compatible PC. The atomic orbital parameters[23] employed in the calculations are summarized in Table 2. A 60 k-point mesh was used for calculations on the primitive orthorhombic structure.

Results and Discussion

The most familiar and more salt-like compounds between tin and the alkaline-earth metals plus magnesium (A) are the relatively straightforward inverse-CaF_2 and the Co_2Si (~$PbCl_2$) types for A_2Sn compositions. But a marked tendency for Sn−Sn bonding is also evident. Traditional examples include the rather standard SrSn (but not CaSn) with the CrB-type structure (infinite zigzag chains of tin) and Sr_5Sn_3 (Cr_5B_3-type with Sn dimers).[24] Some more remarkable compounds listed in the Introduction utilize alkali-metal cations instead. These and others illustrate the remarkable degree to which the number, size, and charge of the cations, important variables in achieving efficient packing and energetically favorable covalent bonding and Coulombic interactions in crystalline solids, may influence phase stability and structure. Recently, the utilization of mixtures of cations of different sizes has been shown to be a powerful means for the synthesis of new and novel anionic clusters and networks. This has been demonstrated particularly well in alkali-metal−thallium systems in which seven of ten "naked" polythallium cluster types have been discovered only in the presence of the subtly altered packing afforded by mixed

(18) TEXSAN, version 6.0 package, Molecular Structure Corp.: The Woodlands, TX 1990.
(19) SHELXS-86, Sheldrick, G. M.; Universität Göttingen, Germany, 1986.
(20) Shinar, J.; Dehnar, B.; Beaudry, B. J.; Peterson, D. T. *Phys. Rev.* **1988**, *B37*, 2066.
(21) Whangbo, M.-H.; Hoffmann, R. *J. Am. Chem. Soc.* **1978**, *100*, 6093.
(22) Ammeter, J. H.; Birgi, H.-B.; Thibeault, J.; Hoffmann, R. *J. Am. Chem. Soc.* **1978**, *100*, 3686.
(23) Vela, A.; Gázquez, J. L. *J. Phys. Chem.* **1988**, *92*, 5688.
(24) Villars, P.; Calvert. L. D. *Pearson's Handbook of Crystallographic Data for Intermetallic Phases*, 2nd ed.; American Society for Metals International: Metals Park, OH, 1991.

Table 3. Positional and Isotropic-Equivalent Thermal Parameters for $Ca_{6.24(6)}Mg_{3.76(6)}Sn_7$

atom	*x*	*y*	*z*	B_{eq}[a]
Sn1	0.6110(2)	0.12313(5)	1/2	0.84(6)
Sn2	0.0842(2)	0.20498(6)	0	0.82(6)
Sn3	0.1214(2)	0.04056(5)	1/2	0.82(6)
Sn4	1/2	0	1/2	1.4(1)
Ca1	0.8038(6)	0.0491(2)	0	1.1(2)
Ca2	0.3327(5)	0.0984(2)	0	1.1(2)
Ca3	0.3689(5)	0.2258(2)	1/2	1.0(2)
Mg1/Ca4[b]	0.7072(8)	0.1858(3)	0	0.9(3)
Mg2	0.9848(9)	0.1446(3)	1/2	0.9(3)

[a] $B_{eq} = (8\pi^2/3)\sum_i\sum_j U_{ij}a_i^*a_j^*\vec{a}_i\vec{a}_j$. [b] With 0.88(3)/0.12(3) proportions.

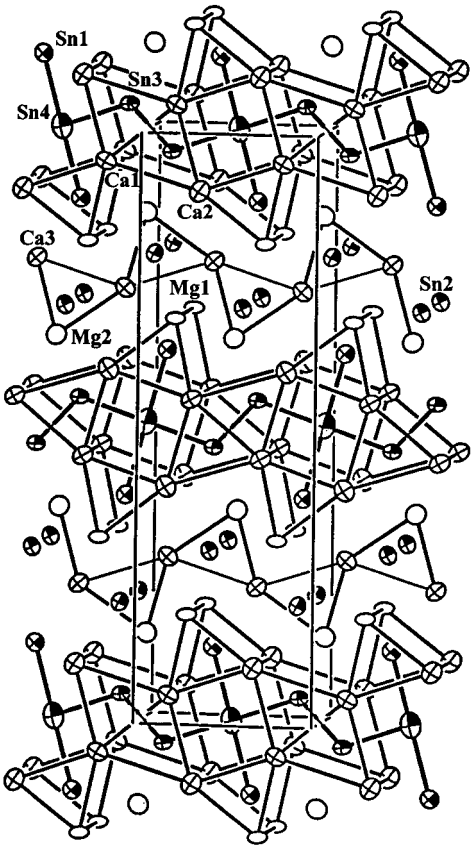

Figure 1. Off-[001] section of the orthorhombic unit cell of $Ca_{6.2}Mg_{3.8}Sn_7$ down the short (4.655 Å) axis with $\vec{b}$ vertical; 98% ellipsoids. All atoms lie at $z = 0$ or $^1/_2$, and the two types of chains that run along $\vec{a}$ are alternately displaced by $c/2$. The Sn atoms are quarter-shaded, Ca atoms crossed, and Mg atoms open, with one atom of each type numbered. Sn−Sn bonds are emphasized.

cations.[26,27] The same is found here for the remarkable $Ca_{6.4}Mg_{3.6}Sn_7$, for which the positional data are given in Table 3.

Structure. The ∼[001] section of the structure in Figure 1 shows how the structure is built basically of trigonal prisms of Ca and Mg (crossed and open ellipsoids, respectively) centered by Sn (quarter-shaded). All atoms in the structure lie at $z = 0$ or $^1/_2$ in this projection along the short axis (4.655 Å), and the trigonal prisms shown also share their triangular faces to generate an infinite structure normal to the figure. Two different chains of trigonal prisms that run along $\vec{a}$ (horizontal) contain the important features. Those that are centered by Sn at $z = 0$, 1 run along $y = ^1/_4, ^3/_4$ and consist of a single type of prism built of Ca3 and Mg2 that share two Ca−Ca side edges to generate infinite zigzag chains. These are centered by isolated Sn2 atoms (d(Sn−Sn) > 4.0 Å) that have formal −4 oxidation states. The other more significant chains alternate along $y = 0, ^1/_2$ and enclose the zigzag planar chains of tin at $z = ^1/_2$. This chain can be generated as follows: Four trigonal prisms alternately centered by Sn1 and Sn3 share Ca−Ca edges to generate a slightly distorted cube of Ca1 and Ca2 atoms that is centered by Sn4. The outward directed, unshared vertexes of two opposed prisms on the faces of this cube that contain Sn1 are the mixed cationic sites, ∼88% Mg1 and 12% Ca4. The other pair of prisms associated with this cube are built of only Ca and contain Sn3, and both Sn3 and the foregoing Sn1 are bonded to the central Sn4 through the side faces of the cube to generate the square-planar Sn_5 arrangement. The prisms about Sn3 share faces with adjoining like assemblies to generate both Sn3−Sn3 bonds through the faces of these trigonal prisms and the zigzag chains of interlinked Sn_5 units. Distances in the chains (Table 4) are as follows (in Å):

$$^1_\infty\{\overset{2.82}{-}Sn3\overset{3.13}{-}Sn4(\overset{3.28}{-}Sn1)_2\overset{3.13}{-}Sn3\}$$

In comparison, separations between one- and two-bonded atoms in the oligomers in $Ca_{31}Sn_{20}$ are 3.06−3.15 Å,[13] where some matrix effects and charge repulsions might be expected, while those within the four-bonded tin array in K_8Sn_{25} are 2.81−2.86 Å,[14] suggesting the comparable Sn3−Sn3 here is a reasonable single bond. The nonclassical bonding of square-planar Sn4 and the other disparate bond lengths will be considered later. The actual bonding around Sn4 is of course only D_{2h} owing to the 0.15 Å difference in bonds to the outer Sn atoms and an Sn1−Sn4−Sn3 angle of 85°.

Table 4. Important Bond Distances in $Ca_{6.24(6)}Mg_{3.76(6)}Sn_7$

Sn1−Sn4		3.283(1)	Mg2−Sn1		2.965(7)
Sn1−Mg1(Ca)	×2	2.929(4)	Mg2−Sn2	×2	2.902(4)
Sn1−Mg2		2.965(7)	Mg2−Sn3		2.881(7)
Sn1−Ca1	×2	3.361(4)	Mg2−Mg1(Ca)	×2	3.349(7)
Sn1−Ca2	×2	3.241(1)	Mg2−Ca1	×2	3.666(7)
Sn1−Ca3		3.245(5)	Mg2−Ca2	×2	3.770(6)
			Mg2−Ca3		3.452(8)
Sn2−Mg1(Ca)		2.979(7)	Mg2−Ca3		3.649(8)
Sn2−Mg1(Ca)		2.968(7)			
Sn2−Mg2	×2	2.902(4)	Ca1−Sn1	×2	3.361(4)
Sn2−Ca2		3.359(4)	Ca1−Sn3	×2	3.405(4)
Sn2−Ca3	×2	3.377(3)	Ca1−Sn3	×2	3.328(4)
Sn2−Ca3	×2	3.260(3)	Ca1−Sn4	×4	3.552(4)
			Ca1−Mg1(Ca)		3.595(8)
Sn3−Sn3		2.817(3)	Ca1−Mg2	×2	3.666(7)
Sn3−Sn4		3.130(2)	Ca1−Ca1		3.967(9)
Sn3−Ca1	×2	3.405(4)	Ca1−Ca2		3.879(5)
Sn3−Ca1	×2	3.328(4)	Ca1−Ca2		3.942(6)
Sn3−Ca2	×2	3.218(3)			
Sn3−Mg2		2.881(7)	Ca2−Sn1	×2	3.241(1)
			Ca2−Sn2		3.359(4)
Sn4−Sn1	×2	3.283(1)	Ca2−Sn3	×2	3.218(3)
Sn4−Sn3	×2	3.130(2)	Ca2−Sn4	×4	3.675(3)
Sn4−Ca1	×4	3.552(4)	Ca2−Ca1		3.879(5)
Sn4−Ca2	×4	3.675(3)	Ca2−Ca2		3.942(6)
			Ca2−Mg1(Ca)		3.680(7)
Mg1(Ca)−Sn2		2.968(7)	Ca2−Mg2	×2	3.770(6)
Mg1(Ca)−Sn2		2.979(7)			
Mg1(Ca)−Sn1	×2	2.929(4)	Ca3−Sn1		3.245(5)
Mg1(Ca)−Ca1		3.595(8)	Ca3−Sn2	×2	3.260(3)
Mg1(Ca)−Ca2		3.680(7)	Ca3−Sn2	×2	3.377(3)
Mg1(Ca)−Ca3	×2	3.489(6)	Ca3−Mg1(Ca)	×2	3.664(6)
Mg1(Ca)−Ca3	×2	3.664(6)	Ca3−Mg1(Ca)	×2	3.489(6)
Mg1(Ca)−Mg2	×2	3.349(7)	Ca3−Mg2		3.452(8)
			Ca3−Mg2		3.649(8)

(25) Dong, Z.-C.; Corbett, J. D. *J. Am. Chem. Soc.* **1995**, *117*, 6447.
(26) Corbett, J. D. In *Chemistry, Structure and Bonding of Zintl Phases and Ions*; Kauzlarich, S. M., Ed.; VCH: New York, 1996; Chapter 3.
(27) Corbett, J. D. *Structure Bonding* **1997**, *87*, 157.

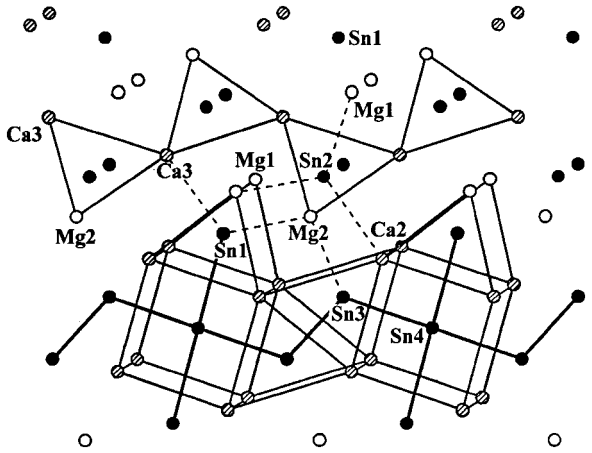

Figure 2. A detail of Figure 1 that marks with dashed lines all examples of the augmented bonding of tin atoms to further cations through the faces of the trigonal prisms. These bonds are close in length to those within prisms, all are between the horizonal chains in Figure 1, and most involve Mg (Sn, solid; Ca, striped; Mg, open).

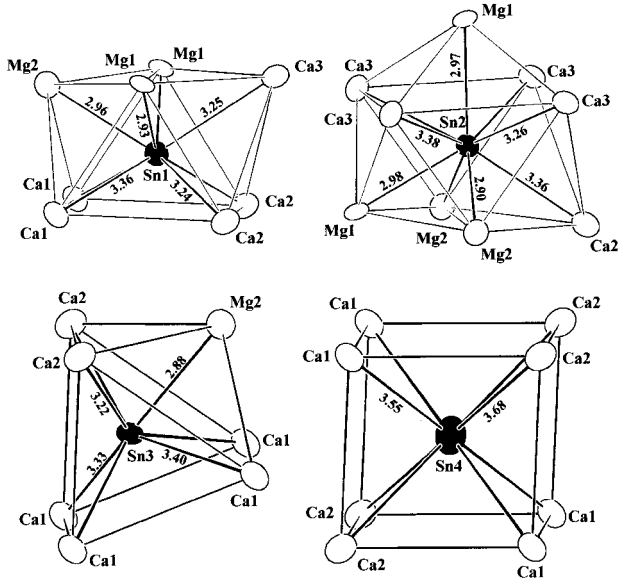

Figure 3. The cation polyhedra around each of the tin atoms as viewed roughly along $\vec{c}$, without Sn−Sn bonding. Only Sn4 lies at a point of higher symmetry, 2/*m*.

Further aggregation of the chain structure depicted in Figure 1 is also present. Augmentation of trigonal prismatic coordination about the centered atom by additional cation neighbors beyond the prism faces is a common motif in most constructions of this type.[28] Figure 2, a small section of Figure 1 around $y \sim 0.65$, shows with dashed lines the location of these additional Sn−cation interactions. The two types of chains noted earlier are in fact strongly interbridged by just these additional bonds, contrary to the impression given by Figure 1. Tin atoms 1, 2, and 3 have two, three, and one such additional contact, respectively, and four of the six involve magnesium cations. Distances for these additional bonds are very similar to those present for the same atom types elsewhere in the structure. For completeness the entire polyhedron about each Sn, which is also not marked in Figure 1 for purposes of clarity, is separately illustrated in Figure 3.

Since this structure does not exist with only calcium cations, the magnesium component must be essential in achieving the increased coordination number for tin and in the "fit" of the structural pieces, and Figure 2 gives some good evidence for this. (Yb−Mg−Sn could be another interesting case.) While calcium atoms 1, 2, and 3 have 10, 9, and 5 Sn neighbors, respectively, Mg1 (with 12% Ca) and Mg2 bond to only 4 Sn atoms each, half in the other chain. Thus we are led to the conclusion that Mg is really essential to the interchain bonding, and the shorter Mg−Sn interactions might be expected to be stronger than Ca−Sn. The predominant Ca−Sn bond types in this structure average 3.31 Å, in contrast to the 3.61 Å in the large cube around Sn4 where the Sn−Sn bonds through the faces are also longer, for good reason (later). The former are typical of those in other Ca−Sn phases, and the same pertains to the Mg−Sn separations. The closest analogue to this general structure is the inverse-$PbCl_2$-type.[28]

Properties. Polycrystalline $Ca_{6.4}Mg_{3.6}Sn_7$ appears to be a good metallic conductor and is weakly diamagnetic. The measured specific resistivities increase from about 12 to 22 $\mu\Omega\cdot$cm over the range of 90−260 K (0.3% K^{-1}), distinctly smaller resistivities than found in metallic Zintl phases containing In or Tl.[26] (On the other hand, the clearly closed-shell network phases K_8Sn_{25} and K_8Sn_{44} are semiconducting and diamagnetic.) $Ca_{6.4}M_{3.6}Sn_7$ exhibits a weak and essentially temperature-independent diamagnetism of 4×10^{-5} emu mol^{-1} over ∼65−300 K, or only 3×10^{-8} emu g^{-1} when the large formula mass is taken into account. (Both sets of experimental data are illustrated in the Supporting Information.) The weakly diamagnetic signal for a metallic compound appears consistent with the somewhat classical but nontraditional characteristics of heavier p elements (In, Tl, Bi for example) and some of their compounds. This behavior has been attributed to the small effective electron masses arising from high DOS at E_F and large orbitals for the metals or metametals.[29]

Bonding. Naive counting of the bonding electrons (oxidation states) according to the classical Zintl−Klemm octet bonding scheme[30] for the tin atom arrangement in $Ca_{6.2}Mg_{3.8}Sn_7$ (one 4b- (four-bonded) Sn4°, two 2b-$Sn3^{2-}$, two 1b-$Sn1^{3-}$, and two 0b-$Sn2^{4-}$ per formula unit) gives a total of 18, two fewer than the 20 e^- afforded by the 10 metal cations. This difference arises because of the electron-richer nature of the four-bonded tin atom in a square-planar environment.

To account for this mismatch and to better understand both the bonding and the interrelations between the structure and the observed properties, electronic band structure calculations were carried out on the observed tin chain substructure as well as on the complete structure. The band structure resulting from a one-dimensional calculation on the $^1_\infty[(Sn3)_2Sn4(Sn1)_2]$ chain is depicted in Figure 4. The Fermi level E_F marked by an arrow is for the $^1_\infty[Sn_5^{10-}]$ formulation that results from the above (questionable) octet assignment $(Sn4^0)(Sn3^{2-})_2(Sn1^{3-})_2$. This lies immediately below another band A above which a 2 eV gap to band B exists. Filling A would require two more electrons per Sn_5 unit ($^1_\infty[Sn_5^{12-}]$) and give a Fermi level at −5.29 eV, which then matches expectations from the oxidation state count for the overall structure (with 10 A^{2+} cations and two isolated $Sn2^{4-}$). (Of course, actual charges would not be expected to be nearly as large as these formally assigned oxidation states.)

The main orbital characters of bands A and B at Γ and X (a^*/2,0,0) are shown in Figure 5. Those for the occupied band A are π-type, nonbonding around Sn4 and antibonding for Sn3−

(28) Hyde, B. G.; Andersson, S. *Inorganic Crystal Structures*; Wiley: New York, 1989; p 80ff.

(29) Seitz, F. *Modern Theory of Solids*; Dover: New York, 1987; p 590.

(30) Kauzlarich, S. M., Ed. *Chemistry, Structure and Bonding of Zintl Phases and Ions*; VCH: New York, 1996.

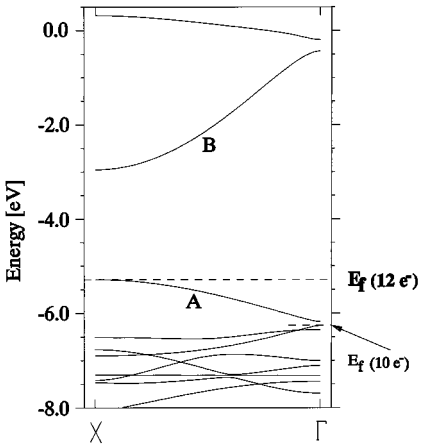

Figure 4. Band structure diagram according to a one-dimensional extended Hückel calculation for the isolated $^1_\infty[Sn_5]$ chain in $Ca_{6.2}Mg_{3.8}Sn_7$. The Fermi levels for charges of 10 (classical) and 12 e^- (actual) per Sn_5 unit are marked. The observed HOMO and LUMO bands are labeled A and B, respectively.

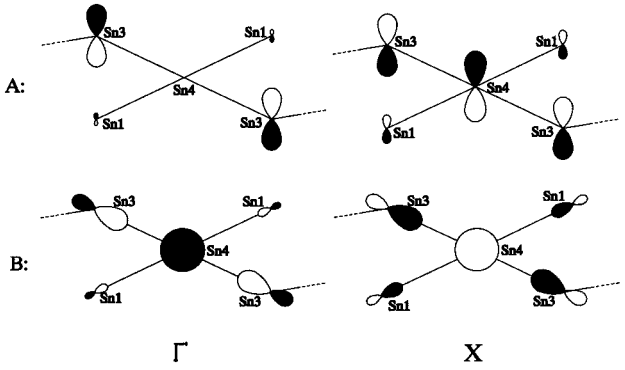

Figure 5. Orbital contributions to bands A and B for the $^1_\infty[Sn_5^{12-}]$ chain at the high symmetry points Γ and X.

Sn3 at Γ, and antibonding around Sn4 and bonding for Sn3−Sn3 at X (along the chain in reciprocal space). In contrast, the LUMO band B is of σ-type and is antibonding around Sn4 and bonding for Sn3−Sn3 at both Γ and X. An MO calculation on the equivalent isolated Sn_5^{14-} subunit (D_{2h}) yields a b_{1u} HOMO orbital that is basically identical to that for band A at point X for the infinite chains, and an a_g LUMO very much like band B at X, Figure 5. Thus, band A can best be described as an extended delocalized analogue of a local p_z^2 lone pair on the Sn4 atom in the square-planar Sn_5 unit. The analogy can be carried further by noting that Sn_5^{14-} is isoelectronic with XeF_4^{2+} and with the 10-electron SnH_4^{2-} where only σ orbitals are present on the outer atoms.[31] The σ bonding manifold (in D_{4h}, omitting significant s−p mixing) then contains the 5-center a_{1g}^2 (s on Sn4), the 3-center e_u^4 (p_x, p_y), the 4-center b_{1g}^2 only on the outer "ligands", the hyperelectronic characteristic, and the a_{2u} HOMO (p_z^2), while the antibonding version of the first a_{1g}* is the LUMO. Again, the last two are seen qualitatively in Figure 5 for bands A and B at X, respectively. The Sn_5^{14-} center thus represents the first example of an intermediate degree of hypervalency in which only one electron pair is delocalized on the outer ligands rather than the normal two. Related, maximally hypervalent square-planar units have been thoroughly described for a series of compounds containing Te_5^{n-} anions.[32] The formation of the present bonding situation, a quite

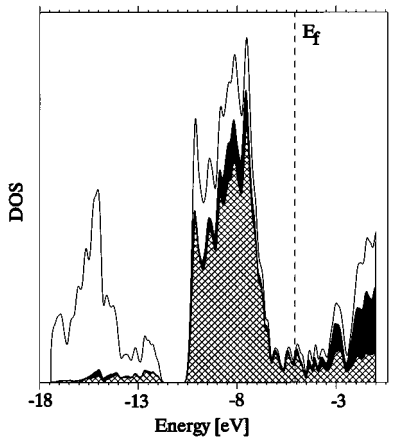

Figure 6. Densities of states diagram from a full band calculation on $Ca_{6.2}Mg_{3.8}Sn_7$. The separate Sn 5p contributions (hatched) and Ca 4p contributions (solid) are projected out.

complicated problem, must arise in part from the strongly reducing active metals and the substantial stabilizing Madelung energy they afford, an efficiently packed structure, and a situation where the interbonded atoms are not particularly electronegative. All four tin atoms must be electronically distinctive in this respect, although we have not attempted to include this in these relatively simple calculations.

The distribution of intermediate hypervalent bonding among the chain atoms is reasonably reflected in distances: the distinctly longer Sn4−Sn1 (3.28 Å) and Sn4−Sn3 (3.13 Å) bonds within the D_{2h} "square" relative to the plausible single bond distance of 2.82 Å for Sn3−Sn3 noted before. The overlap populations vary inversely with these distances in an appropriate manner, 0.282, 0.365, and 0.623, respectively (from the full solid calculation, below). Significant matrix effects from the imposed cation lattice that could influence these distances seem plausible as well, including from the greater number of Mg neighbors around Sn1. In analogy to the results of calculations on Te_5^{n-} units,[32] there is no driving force for the square-planar (D_{2h}) Sn_5 unit to distort locally toward C_{2v}, as there is in SF_4.[31] The calculated Walsh diagram illustrating this is contained in the Supporting Information.

To visualize the effects of the cations on the electronic band structure and to compare observed properties with theoretical predictions, three-dimensional calculations were also performed on the complete structure including the cations (with the mixed Mg1/Ca4 site completely occupied by Mg). The total densities of states (DOS) plot is shown in Figure 6 together with separate projections for the Sn p and Ca p orbital contributions. The block of states at lower energy originates largely from s orbitals and is clearly separated by ∼1.8 eV from p-orbital contributions of Sn, Ca, and Mg. The Fermi level at −5.08 eV crosses a region wherein the DOS clearly do not fall to zero and contain appreciable cation contributions, contrary to the result for the isolated chain.

The band structure of this system along high-symmetry lines around the Fermi level is depicted in Figure 7A. The symbols for the high symmetry points employed in Figures 4 and 7 are indicated on the insert of the Brillouin zone (Γ = (0, 0, 0); X = (a*/2, 0, 0); Y = (0, b*/2, 0); Z = (0, 0, c*/2); Σ = (a*/2, 0, c*/2); T = (0, b*/2, c*/2)).[33] Because there are two formula units per cell, each band appears twice. Along Γ→X the Fermi level clearly cuts through four bands. Another pair of cuts may

(31) Albright, T. A.; Burdett, J. K.; Whangbo, M. H. *Orbital Interactions in Chemistry*; J. Wiley: New York, 1985; pp 263 and 271.

(32) Bernstein, J.; Hoffmann R. *Inorg. Chem.* **1985**, *24*, 4100 and references therein.

(33) Miller, S. C.; Love, W. F. *Tables of Irreproducible Representations of Space Groups and Co−Representations of Magnetic Space Groups*; Pruett Press: Boulder, CO, 1967.

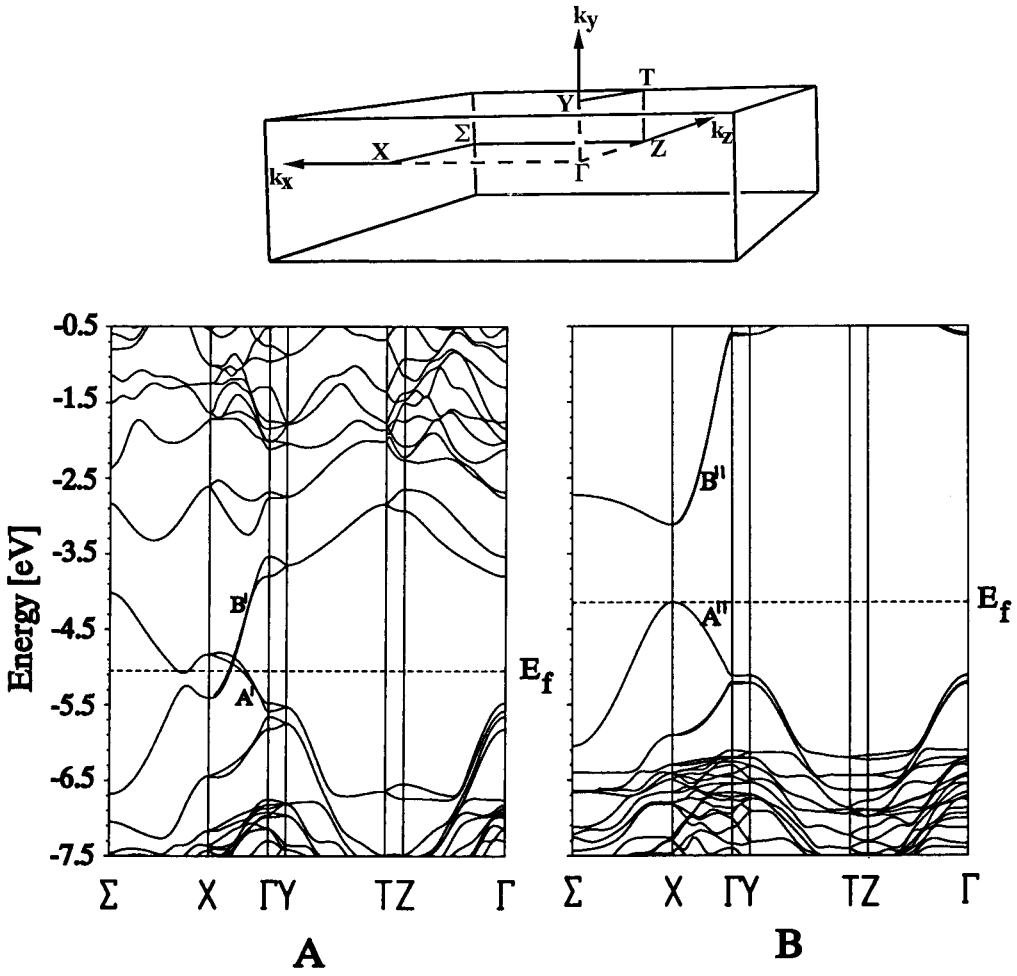

Figure 7. Band dispersions resulting from three-dimensional calculations on both the complete $Ca_{6.2}Mg_{3.8}Sn_7$ structure (A) and the cation-free tin substructure (B) with the Fermi levels E_F as dashed lines. The equivalents to the A and B bands in Figure 5 are marked with single and double primes, respectively.

occur through the bottom part of a doubly degenerate band along Σ→X. Since the collection of band cuts occurs in two orthogonal directions in the Brillouin zone, and the band dispersion along the Γ→Y direction (interchain in real space) is small, the EH band results suggest this material is a two-dimensional metal—a general metallic property being confirmed by measurements on a powdered sample (above). The similarity of the (double) bands along X→Γ around E_F to those resulting from the 1-D calculation on the Sn_5 chain, Figure 4, is evident, indicating that they are largely Sn in character. The major difference between the 1-D Sn_5 chain result and the 3-D structure is that the lowest unoccupied band in the former (B) has moved down and closed the band gap in the real structure. An analysis of the orbital character of band B′, Figure 7A, shows that it is of σ-type (Figure 5), and therefore the crossing of bands A′ and B′ just above the Fermi level is symmetry-allowed. The pronounced decrease in energy from B to B′ largely results from p_x and p_y orbital contributions by Ca2 and Ca3, whereas the atoms in the mixed Mg1(Ca) site have a negligible contribution to B′. To confirm the latter, another calculation was done with this site completely occupied by Ca. The resulting orbital components of this band as well as the energies changed by only vanishingly small amounts. Although the mixed occupation of this site may be important as far as size, it does not play a role in the electronic structure in the vicinity of the Fermi level and therefore in the conduction properties as well.

To see the influence of cations on the band-shapes, the three-dimensional band structure without cations was also calculated (Figure 7B). A general lowering of the band energies from cation mixing is evident in Figure 7A, the substantial drop between B″ and B′ (or B) arising from the cation mixing noted above. Another interesting feature of both band structures in Figure 7 is the generally strong dispersion of the bands only along the X→Γ, Z→Γ, Y→T, Σ→X directions in the Brillouin zone, that is, within the $a-c$ plane that contains the chains (which runs horizontally and normal to Figure 1). This indicates some direct σ-type interactions occur not only along the chains but also between the p_z orbitals on parallel $^1_\infty[Sn_5]$ chains (along $\vec{c}$) that do not depend on the cations. Even though these Sn−Sn distances are quite long (c, 4.655 Å), the rather diffuse 5 p_z orbitals used for tin (if suitable) can evidently have a large influence on the shape of particularly the A band in this direction (compare Figure 4A). The total overlap population for these contacts is −0.11. Similar observations have been made for layered transition metal tellurides.[34]

The calculations show that the Ca and Mg cations do not alter the Sn−Sn bonding in this phase in a significant way, rather the bonding arises via direct Sn−Sn interactions along $\vec{a}$ and $\vec{c}$, even though the latter are not very strong. But the cations are essential not only as the glue but also for the compound to be metallic, i.e., for the band crossings at the Fermi level. The bonding thereby revealed in this compound is thus consistent with its classification as a metallic Zintl phase,[26,35] one in which

a gap does not exist but in which covalent bonding at lower energies is of paramount importance in determining the structure.

Finally, it is worth noting again that the simple act of mixing dipositive Ca^{2+} and Mg^{2+} cations allows one to obtain this novel phase with its remarkable tin anion substructure and the unique square-planar bonding about tin. Interestingly, a hypothetical example of square-planar SnH_4 has been used as a pedagogical example for some years.[36] Furthermore, the $^1_\infty[Sn_5]$ chain itself would be closed-shell, a characteristic observed in several other polytin structures, except for mixing of calcium orbitals into the bonding states that makes the solid compound metallic. Marvelous!

Acknowledgment. We are indebted to Enric Canadell, Roald Hoffmann, and Tim Hughbanks for helpful comments.

Supporting Information Available: Tables of additional crystallographic data and anisotropic atomic displacement parameters, a Walsh diagram of the $C_{2h} \rightarrow D_{2h}$ transformation in Sn_5, and plots of resistivity and magnetic susceptibility results (5 pages). See any current masthead page for ordering and Web access instructions.

JA972812+

(34) Canadell, E.; Jobic, S.; Brec, R.; Rouxel, J.; Whangbo, M.-H. *J. Solid State Chem.* **1992**, *99*, 189.
(35) Nesper, R. *Prog. Solid State Chem.* **1990**, *20*, 1.
(36) Albright, T.; Burdett, J. K. *Problems in Molecular Orbital Theory*; Oxford University Press: Oxford, UK, 1992; p 259.